Copyright © 2007 by ABCM

PREDICTION OF BUCKLING BEFAVIOR OF THIN SHELLS BY 3D THERMO_VISCO PLASTIC ANALYSIS

Sima Ziaee, sima_ziaee@yahoo.com
Ph.D student, Department of Mechanical Engineering, School of Engineering, Shiraz University, Shiraz, Iran.
M.H. Kadivar, kadivar-mh@pidec.com
Professor, Department of Mechanical Engineering, School of Engineering, Shiraz University, Shiraz, Iran.

K. Jafarpur, jafarme@shirazu.ac
Associate Professor, Department of Mechanical Engineering, School of Engineering, Shiraz University, Shiraz, Iran.

Abstract. *Welding causes residual stresses in structures which may lead to buckling distortion, if they exceed the critical buckling stress of the structure, This paper presents a predictive distortion analysis approach for welded structure. 3-D thermo-mechanical welding process simulations are performed to determine the residual stress and deformation. The critical buckling stresses along with the buckling mode are computed through a 3-D eigenvalue analysis. The correctness of results is confirmed experimentally. This work clearly show that the proposed 3D analysis welding can predict not only the time of occurance but also the shape of buckling during welding. Also, one is able to see the behavior of shell after buckling. In addition, the effect of external constraint and thickness on the buckling behavior due to welding is also studied.*

Keywords*: Buckling behavior, Anand model, External constraint, Thermo visco-plastic analysis*

1. INTRODUCTION

Welding, among all mechanical joining processes, has been employed at an increasing rate for its advantage in design flexibility, cost saving, reduced overall weight and enhanced structural performance. However, welding induces various types of distortion as discussed in detail by Masubuchi (1980). To study the effect of welding on structural efficiency, and in turn to implement various distortion mitigation techniques, a valid method for predicting welding induced distortion is necessary.

Thinner section components are commonly utilized in fabricating large structures to achieve reduction in overall weight and more controllable manufacturing. However, for structures made of relatively thin components, welding can introduce significant buckling distortion which causes loss of dimensional control, structural integrity and increased fabrication costs due to poor fit-up between panels. A predictive analysis technique can determine the susceptibility of a particular design to buckling distortion.

Welding-induced buckling of thin walled structures has been investigated in greater detail in (Murakawa *et al.* ,1995, Michaleris and Debiccari, 1997, Tsai *et al.* ,1999). Murakawa et al. (1995) presented a methodology to determine the buckling behavior of plates by large elastic deformation FEA and employing inherent strain distributions. Mickaleris et al.(1996,1997,2003) developed a predictive buckling analysis technique for thin section panels, combining decoupled weld process simulations and eigenvalue buckling analysis. Phase transformation and transformation plasticity have also been incorporated in the analysis as recent developments showed (Oddy *et al.,* 1990, Watt *et al.*, 1988).

In this work the 3-D thermo elastic-viscoplastic finite element analysis technique is applied to evaluate welding induced buckling of the welded shell. The results are checked by 3-D eigenvalue simulations and experimental work. Moreover effects of the shell thickness and mechanical constraint are also investigated.

2. MECHANICAL MODEL OF WELDING

The Lagrangian description of body motion is used in the formulation of welding as a thermo-mechanical problem for metals. The displacement $\mathbf{u}(\mathbf{X},t)$ and temperature $\theta(\mathbf{X},t)$ in a weld joint are unknown and the initial position of the particle $\mathbf{X} = (X_1^0, X_2^0, X_3^0)$ and the time t are taken as independent variables. The vector joining the point $\mathbf{X}$ and actual position in the space $\mathbf{x} = (X_1^1, X_2^2, X_3^1)$ is the displacement vector given by $\mathbf{u} = \mathbf{X} - \mathbf{x}$. The constitutive variables, i.e. the stress and strain measures used in the Lagrangian formulation are the second Piola-Kirchoff stress tensor $\mathbf{T}$ and its deviator $\mathbf{S}$, as well as the Green-Lagrange total strain tensor $\mathbf{L}$ and deviator $\mathbf{E}$.

Welding is a coupled thermo-mechanical process and its mathematical model consists of two principles expressing thermal and mechanical equilibrium, i.e. the balance of internal energy and balance of momentum as well as satisfying initial and boundary conditions. The equilibrium condition for a solid is given by the following equations:

$$\begin{aligned} &div(\mathbf{T}+\mathbf{T}\cdot\nabla\mathbf{u})-(\mathbf{b}+\mathbf{r})\rho_0=0 \qquad &&for\ particle\ \mathbf{X}\in\boldsymbol{\Omega}\\ &\mathbf{N}\cdot(\mathbf{T}+\mathbf{T}\cdot\nabla u)=\widetilde{\mathbf{T}} \qquad &&for\ particle\ \mathbf{X}\in\partial\boldsymbol{\Omega}\end{aligned} \tag{1}$$

where $\nabla \equiv N^J \partial / \partial X^J$, and the comma "," is the usual abbreviated notation for a gradient component. The balance of internal energy for a non-rigid conductor can be expressed in the form of:

$$\rho\dot{e} + div\mathbf{q} = \mathbf{T} : \dot{\mathbf{L}} + {}_{ext}\mathbf{q}\cdot\mathbf{N} + \rho R \tag{2}$$

where e is the energy density per unit mass, $\mathbf{q}$ is the vector of heat flux transferred through the particle $\mathbf{X}\in\boldsymbol{\Omega}$, ${}_{ext}\mathbf{q}$ is the heat flux supplied to the welded body through the outer surface $\partial\boldsymbol{\Omega}$, and R is heat losses through radiation. By considering thermal homogeneity for the welded material and after some manipulations, the indicial form of equation of internal energy balance could be rewritten as a function of temperature θ (Ronda and Oliver, 1998):

$$C\dot{\theta} + K_{IJ}\theta_{,JI} = f_\theta^B + f_\theta^S + \sum_\varsigma F_\theta^\varsigma \tag{3}$$

where

$f_\theta^B = T_{IJ}\dot{L}_{IJ}$ rate of heat generation due to mechanical energy dissipation in weldments

$f_\theta^S = {}_{ext}q_J N_J + \rho R$ heat flux of welding arc and out – fluxes due to convection and radiation

$C = \rho_0 C_V$ constant volume specific heat

$\sum_\tau \mathrm{F}_\theta^\tau$ Concentrated heat fluxes

In the above equation, f_θ^B plays the role of thermo-mechanical coupling between the mechanical and thermal systems. The magnitude of this term in welding is very small compared to the heat energy of arc and has a negligible effect on thermal history of plates (Argyris *et al.*, 1982, Hong, *et al.*, 1998, Sarkani *et al.*, 2000). Due to this approximation, some investigators have neglected its effect. This assumption makes the problem to be thermo-mechanically uncoupled. Then, two separate analysis, thermal and mechanical analysis have been performed.

2-1-Finite element approximation

The finite element method for the fully coupled thermo-mechanical problem is based on the Ritz's approximation of variational equation, i.e. the principle of virtual work and the balance of internal energy.

The combined global finite element equation for the fully coupled thermo-mechanical problem is expressed by

$$\begin{bmatrix} \mathbf{K}_u^n & \mathbf{K}_{u\theta}^n \\ \mathbf{K}_{\theta u}^n & \frac{1}{\Delta t}\mathbf{C}^n + \mathbf{K}_\theta^n \end{bmatrix} \begin{bmatrix} \Delta\mathbf{u} \\ \Delta\theta \end{bmatrix}^i = \begin{bmatrix} \mathbf{R}_u^{n+1} \\ \mathbf{R}_\theta^{n+1} \end{bmatrix} - \begin{bmatrix} \mathbf{F}_u^{n+1} \\ \mathbf{F}_\theta^{n+1} \end{bmatrix}^{(i-1)} \tag{4}$$

where $\mathbf{K}_u^n$ is the stiffness matrix corresponding to mechanical effects, $\mathbf{K}_{u\theta}^n$ is the matrix which transforms thermal energy into mechanical one, and $\mathbf{K}_{\theta u}^n$ transforms mechanical energy into the thermal one. The thermal stiffness $\mathbf{K}_\theta^n$ is the sum of stiffness matrix corresponding to conduction, the stiffness related to convection phenomena, and the stiffness associated with radiation effects. $\Delta\mathbf{u}|_{(i)}$ and $\Delta\theta|_i$ are the vector of displacement and temperature increments respectively, $\mathbf{R}_u^{n+1}$ is the vector of externally applied nodal point loads, $\mathbf{F}_u{}^{n+1}|_{i-1}$ is the vector of nodal point forces equivalent to the internal stresses. $\mathbf{R}_\theta^{n+1}$ is the summation of vectors of nodal thermal loads correspond to the thermal conditions. $\mathbf{F}_\theta^{n+1}|_{i-1}$ is the vector of nodal thermal loads correspond to the heat flux through the body surface(Ronda and Oliver, 1998) .

The matrixes in equation (4) are taken at the current, n+1, and previous, n, time steps and current, (i), and previous, (i-1) iterations at the current time step.

The nonlinear FM system of equations is solved iteratively by the Newton-Raphson scheme.

Copyright © 2007 by ABCM

After neglecting the effect of f_θ^B, the stiffness matrices $K_{\theta u}^n$ becomes zero. This will happen because f_θ^B which is equal to $\mathbf{T}:\dot{\mathbf{L}}$ plays the role of thermo-mechanical coupling between the mechanical and thermal systems. Then, after the uncoupled finite element equations for thermo-mechanical problem are obtained after f_θ^B is being omitted.

2-2 –Mechanical model

If transient thermal stresses produced in welding are completely elastic and no incompatible strains are formed, no residual stresses will remain. However, plastic strains are formed in the region around the weld. In this region, temperature rapidly increases and reaches near the melting point of the material. At high temperatures, yield strength of metals reduces. Therefore, transient thermal stresses exceed the yield point of the material, and weldment undergoes plastic deformation. In addition, material is at high homologous temperature in this region, and experiencing rapid temperature changes, could result high thermal strain rate. Thus, rate dependent effects are relatively significant. For these reasons, thermoelastic-viscoplastic model is used to simulate the material behavior.

A simple set of constitutive equations for large, isotropic, visco-plastic deformations is the single-scalar internal variable model proposed by Anand (1989). Two basic features exist in Anand model. First, this model needs no explicit yield condition and no loading-unloading criterion. Second, this model employs a single scalar as an internal variable to represent the averaged isotropic resistance to plastic flow. The inelastic strain rate $\dot{E}^P$ for Anand model is defined by (Ronda and Oliver, 1998):

$$\dot{\mathbf{E}}^P \equiv \tilde{\mathbf{E}}^P(\mathbf{S}, z_1) = \dot{\varepsilon}^P \frac{\mathbf{S}}{\|\mathbf{S}\|}$$
$$\dot{\varepsilon}^P = \tilde{\varepsilon}^P(\mathbf{S}, z_1) = A\exp\left(-\frac{Q}{R\theta}\right)\left[\sinh\left(\xi\frac{\|\mathbf{S}\|}{z_1}\right)\right]^{\frac{1}{m}} \tag{5}$$

where the constitutive function $\tilde{\varepsilon}^P$ was proposed by Anand (1989). Evolution equations for the internal variable z_1 are given by [11]:

$$\dot{z}_1 = h_0\left[1-\frac{z_1}{z^*}\right]^a \dot{\varepsilon}^P \qquad for \quad z_1 \le z^*$$
$$\dot{z}_1 = -h_0\left[\frac{z_1}{z^*}-1\right]^a \dot{\varepsilon}^P \qquad for \quad z_1 \succ z^* \tag{6}$$

with the criterion number

$$z^* = \bar{z}\left[\frac{\dot{\varepsilon}^P}{A}\exp\left(-\frac{Q}{R\theta}\right)\right]^\eta$$

where $A, Q, \xi, m, z, h_0, a, \bar{z}$, and η are constants of Anand model and R is the Boltzman's constant. The material constants for Anand model, which are used in the present work, are listed in table 1.

Table1. Constants of Anand's viscoplastic model for the selected material

Parameter	Value	Unit	Represent:
Q/R	$\frac{175.3}{8.314}$	$\frac{KJ/mole}{KJ/mole\circ K}$	$\frac{Activation\ energy}{Universal\ gas\ content}$
A	1.91e7	Sec^{-1}	Pre-exponential factor
ξ	7	Dimension less	Multiplier of stress
m	0.23348	Dimension less	Strain rate sensitivity of stress
h_0	1115.6	Mpa	Hardening/softening constant
$\bar{z}$	125.1	Mpa	Coefficient for deformation resistance saturation value
η	.07040	Dimension less	Strain rate sensitivity of saturation value
a	1.3	Dimension less	Strain rate sensitivity of hardening/softening

2-3 Thermal model

Because of the small size of melted region (weld pool), the variation of temperature through the pool has a negligible effect on the thermal history of the joining plates. In other words, the temperature of the welding pool is assumed to be uniform and taken as the melting temperature of the welded materials. Due to this assumption, in this work the arc power and its movement were modeled by assuming that the welded region is an isothermal melted pool and this pool has a constant temperature and its location discretely changes with respect to time. In this way, the length of each welded layer, or each welded block, is divided into a number of parts and according to the welding sequence, the location of the melted pool is changed with respect to time. The applied heat is then injected into the weldments in the moving weld pool and transferred from its boundary to the other regions by conducting through the solid materials and convection to the surroundings. During a short time in welding, the welded region remains red-colored and a portion of heat is also dissipated by radiation. In comparison to the two other modes of heat transfer, the part of the arc power transferred by radiation is small, so the effect of this mode of heat transfer is neglected in this study.

Welding time in this work is calculated by dividing the welder speed obtained from the practical welding characteristic data over the length of welded region. The welding lag, inter-pass temperature and the temperature dependent thermal properties of material were also incorporated into the model (table 2).

Table2: variation of material thermal and mechanical properties with temperature

T(C)	Thermal Conductivity k(W/m.K)	Specific Heat C_p(J/kg.K)	Coeff. of Thermal Expansion (10^{-6})	Youngs Modulus E(Gpa)
20	222	904	23.3	72
50	230	930	23.6	72
100	230	930	24	70
150	250	965	25	67
200	260	965	25	67
250	272	985	25	61.5
300	272	980	26	61.5
350	278	1040	26	53
400	278	1100	26	45
450	283	1100	26	45
500	285	1100	26	35
550	285	1100	26	35
600	320	1100	26	17
650	400	1100	26	10
700	400	1100	26	10

2-4-Element birth technique

If material is added to (or removed from) a system, certain elements in the model may become "existent" (or "nonexistent"). The element birth and death options can be used to deactivate or reactivate selected elements in such cases. To achieve the "element death" effect, the program does not actually remove "killed" elements. Instead, it deactivates them by multiplying their stiffness (or conductivity, or other analogous quality) by a severe reduction factor. This factor is usually sets to a small value (order of 10E-6) but can accept other values, as well. Element loads associated with deactivated elements are zeroed out of the load vector. Similarly, mass, damping, specific heat and other such effects are set to zero for deactivated elements. The mass and energy of deactivated elements are not included in summations over the model. An element's strain is also set to zero as soon as that element is deactivated.

In like manner, when elements are "born", they are not actually added to the model; they are simply reactivated. When an element reactivated, its stiffness, mass, element loads, etc return to their full original values. The weld elements in front of the weld are always kept inactive until the front border of the heat source enters the element in the thermal analysis. The element is activated at melting point temperature in the thermal analysis. In the mechanical analysis the elements are kept inactive until the front border of the heat source has passed the inactive element by about one element length. In this analysis, the element is activated with very soft properties (material property at melting point temperature).

2-5 Three-dimensional eigenvalue analysis

The buckling distortion and critical buckling stresses are consequently determined by an eigenvalue analysis through applying the mostly uniform and compressive longitudinal plastic strain field of the weld model on a 3-D structural model as equivalent load.

Copyright © 2007 by ABCM

A constant, negative thermal load is applied at the weld region to introduce the effect of welding into 3-D structure as suggested by Michaleris et al. (1997,2003). Thermal loading is used instead of mapping the plastic strain field, which would required a complex analysis procedure. After that, an eigenvalue analysis is performed to determine the critical residual stresses and buckling distortion. Finally, this value is compared with longitudinal residual stress that is obtained by 2D finite element analysis of welding. Also, the capability of this method to estimate the critical stresses and buckling mode is evaluated by experiments (Michaleris *et al.*, 1997,2003) .

Some investigators estimated the final stress pattern of welded plates by parabola sine curves or the like and used it in a 3D eigenvalue analysis to predict the critical stresses (Masubuchi, 1980). This value is compared with longitudinal residual stress of welded plates. Pattee (1975) examined the ability of this method to estimate the critical stresses experimentally.

These methods only estimate that if the plate buckles or not but no words ever mentioned about the time of buckling and the behavior of plate after buckling.

In this work the actual stress pattern of the shell in each time step is used in a 3D eigenvalue analysis to determine the critical residual stresses and to estimate the time of buckling (during and/ or after opening fixtures). It is used to find a simple way to estimate buckling with a 3D welded analysis. The accuracy of the results are confirmed with experimental data also the final results are compared with two different methods, namely the works of Michaleris (1997,2003) and Pattee (1975).

2-6 Model validation

To confirm the accuracy of the proposed method, a specimen was constructed with a length, width and thickness of L=1800, W= 300, t= 1.5 mm respectively. The symmetrical finite element model was used. Fig.1 shows the variation of longitudinal residual stress of a middle point of shell with respect to time for present model and Pattee's experimental work [10]. As the Fig.1 illustrates, the variation of computed stress has a pattern similar to the pattern of experimental data and shows a good compatibility between the results. Therefore, the procedure presented here is suitable for the analysis of residual stresses and distortions due to welds.

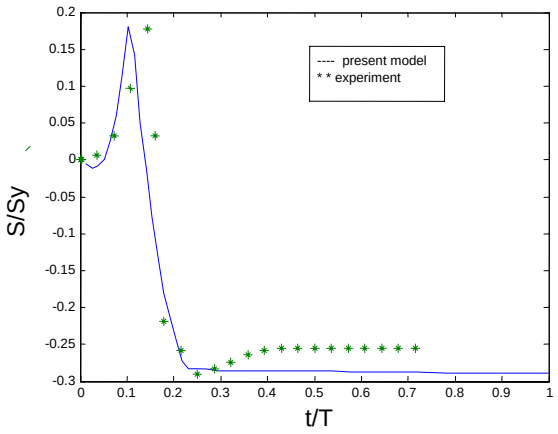

Figure 1: Comparison between present method and experiment.

3- MODEL ANALYSIS

In this work two thin shell sections are jointed by a single pass butt welded. The length, width, thickness and radius of the shell are assumed to be 500, 400, 1.5 (3) and 1000 mm, respectively. The mechanical properties are dependent on the temperature history as listed in table 1. The symmetrical finite element model, that is made with 4000, three-dimensional, 20 nodes elements, is used.

4-RESULTS

To evaluate the response of a welded structure, small elastic deformation eigenvalue analysis is being used. Small deformation analysis requires limited computational resources, and for this reason, it cannot fully predict buckling behavior. However, here, it is only used to estimate stress pattern that causes buckling in each time-step of welding. For this purpose, the true stress pattern of the shell is used in eigenvalue analysis in each time step of welding and the nearest eigenvalue to 1 is selected as buckling time. It is clear that the eigenmode is very similar to the shape of shell at this time.

According to the 3D-eigenvalue analysis, the thin shell has experienced the first buckling mode 36s after the welding has started (λ=0.94). Reviewing the history of deformation would reveal that most of the shell points have a simultaneous and sudden variation in radial direction at the buckling time as Masubuchi (1980) has pointed out [4]. The second buckling occurs at time 60s (λ=1.006) and it is very similar to the first one. For both of them, a sudden jump at the edge of shell and appearance of a new cavity near the weld line are noticeable.

After the second buckling, number of waves in the upper portion of the shell is completed but can not be seen at the edge of shell, also it is not seen any simultaneous and sudden variation again. The history of deformation reveals that after the second buckling, the pattern of deformation changes slightly and the waves move; when the distribution of stresses reaches a stable pattern, they are into their final form (Fig.2). Figure 3 and Fig.4 show estimated final buckling mode by the work of Michaleris (1997, 2003) and experiment respectively. Comparison between Fig.2, 3 and 4 confirmed the accuracy of present analysis.

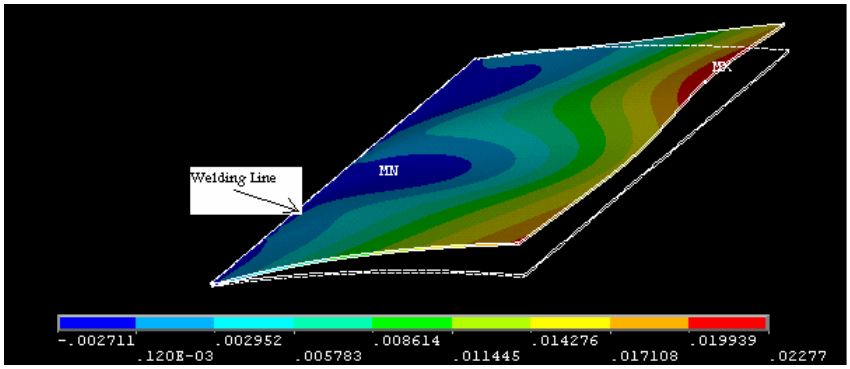

Figure 2a: The final deformed shape of thin shell

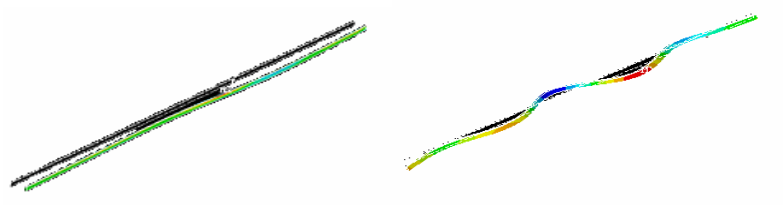

b-1 b-2

Figure 2b: The shape of wave near the edge (b-1) and near the weld line (b-2)

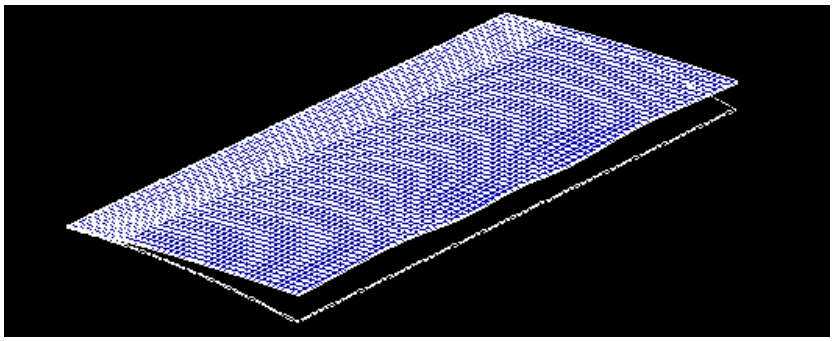

Figure 3: The estimated mode of buckling by the work of Michaleris

Figure 4a: The magnitude of shell jumping

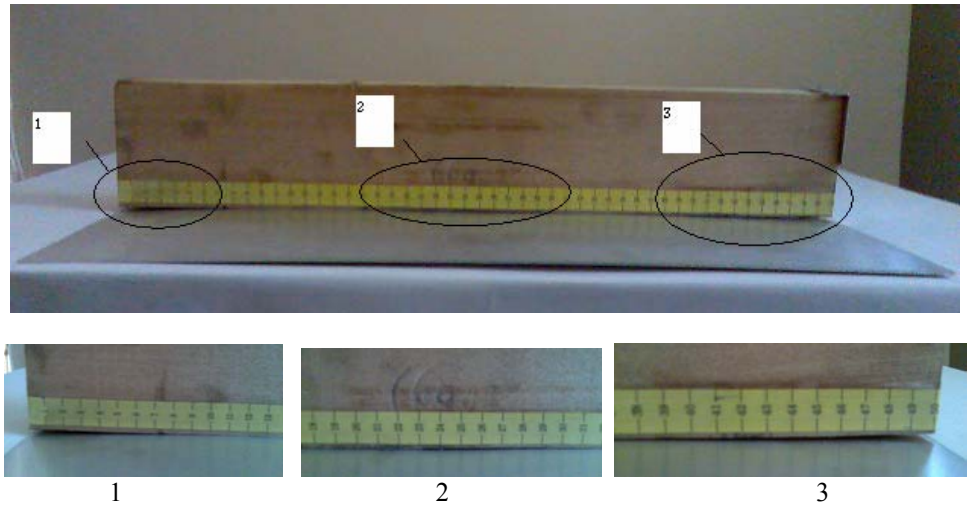

Figure 4b: The shape of waves near weld and near edge.

Twenty seconds after welding has started, simultaneous and sudden variation in radial direction can be observed at a small zone of the shell and one may consider this phenomenon as local buckling and exactly 16s after that the global buckling occurs (Fig. 5). This behavior can be seen at 52s, again (Fig.5).

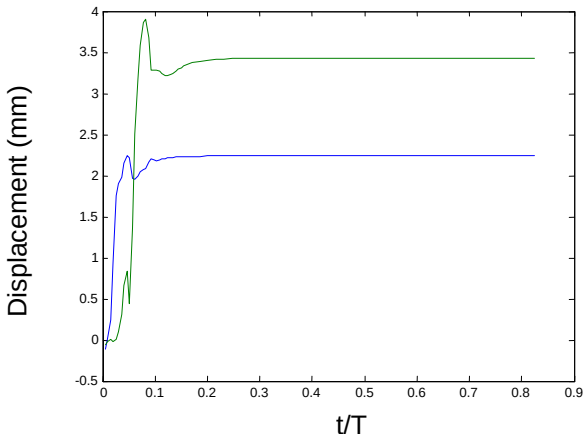

Figure 5: displacement with respect to time of sample node belong to two different local buckling

During the time between the two buckling observation (local/global buckling), the deformation pattern of the shell does not change and only the magnitude of deformations varies.

Examination of the stress pattern illustrates that the nodes experience a negative longitudinal stress at the buckling time but after that it may vary especially at the upper portion of the shell. Figure 6 shows the variation of stress with respect to time for two different points which experience local buckling at different times. These points are on the surface and at the upper portion of the shell (near the weld line).

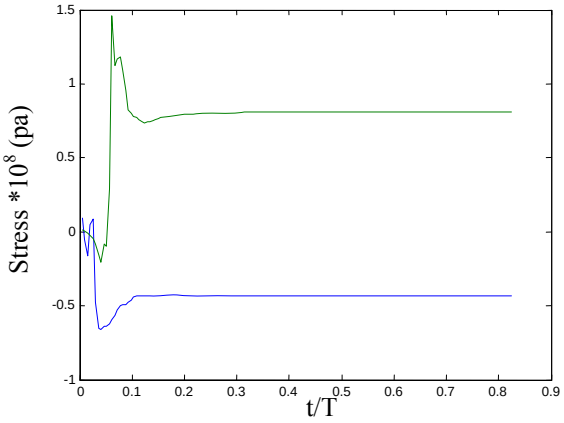

Figure 6: stress with respect to time of sample node belong to two different local buckling

In this work, the effect of external constraint on buckling behavior of thin shells is also studied. Figure 7 shows variation of displacement with respect to time for nodes belong to the upper portion of shell (near the weld line). On the basis of Fig.7, the fixed-fixed shell experiences six different local buckling during the welding. The first one occurs at 4s after the welding has started and the last is at 52s which is coincident with the time of the last buckling of free-free shell.

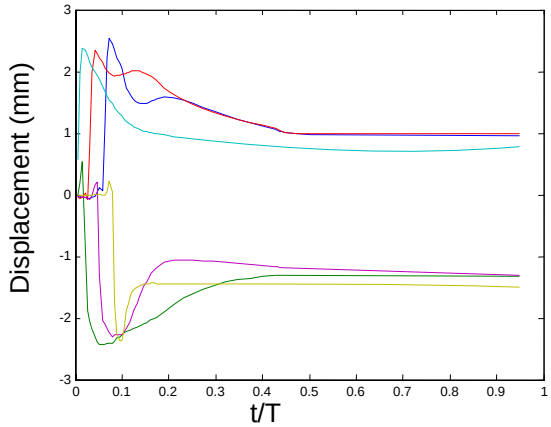

Figure 7: variation of displacement with respect to time for different points near the weld line before releasing the fixtures

Comparison between Fig.5 and 7 illustrates that the shape of first local buckling of fixed-fixed and free-free shell are similar but the last ones are different; one of them is concave and the other is convex. Finally two complete waves are seen on the upper portion of shell. Also the fixed-fixed case experiences its first local buckling sooner and at closer distance from the edge of plate than free-free. At the end of welding, after the shell has been cooled down and the fixtures are released from the sides of the shell, the overall jump is seen that shows the global buckling of shell after cooling (Fig.8).

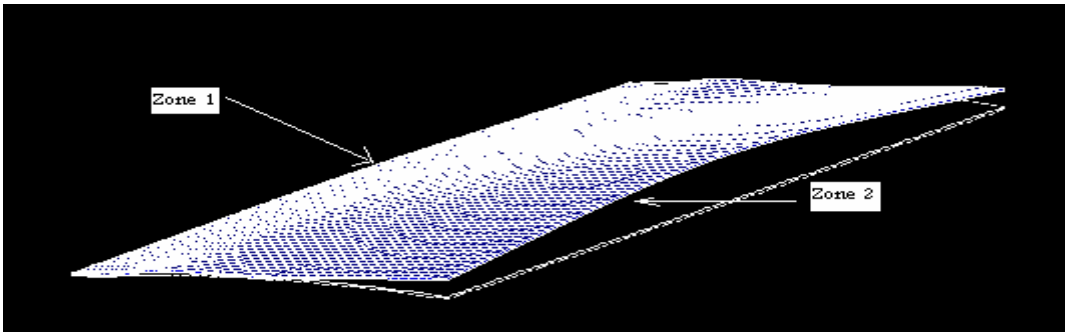

a

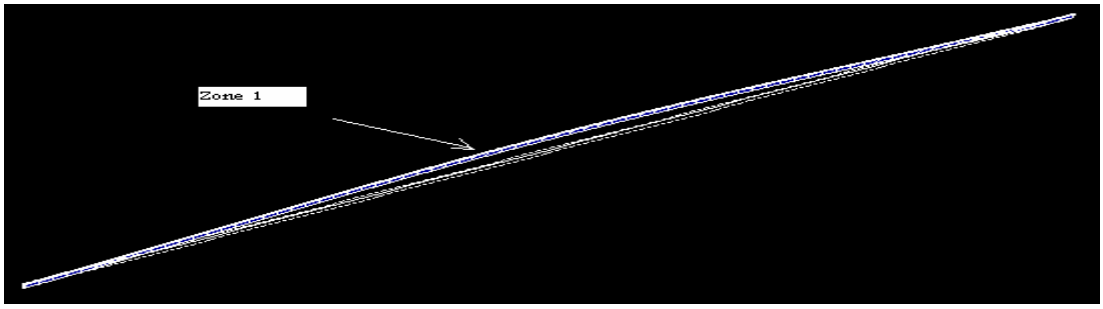

a-1

b

Figure 8: The shape of shell after opening the clamps (free-free condition). a) proposed method b) experiment

As the last example, the buckling behavior of the 3mm shell with fixed-fixed boundary condition is analyzed. By increasing the thickness of shell not only global buckling but also local buckling are eliminated and no jump (overall or local) can be seen during welding and after opening the fixtures (Fig.9).

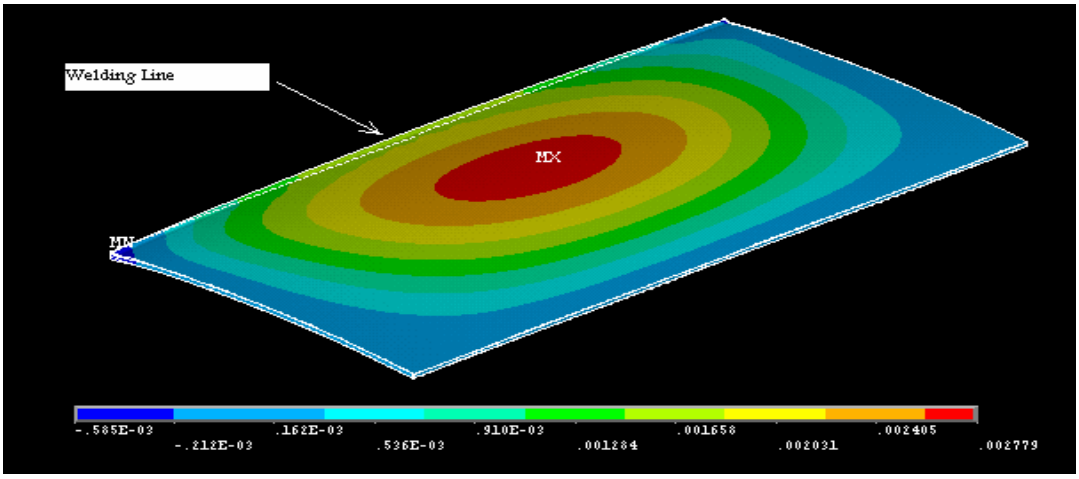

Figure 9: The final deformed shape of 3mm thin shell

Table 3 has summarized the above discussion. Moreover, the results based on Michaleris' method and Pattee's method are also listed.

Table 3: Comparison between present model with two previous models

Case	Average predicted stress before buckling	The first mode critical stress (Michalrris' method)	The first mode critical stress (Pattee' method)	Is case buckled? Estimated/Experiment
Free-free 1.5 mm shell	39Mpa	36.82Mpa	37.5Mpa	Yes/ Yes During welding
Fix-fix 1.5 mm shell	40.3 Mpa	39.02Mpa	21.138Mpa	Yes/ Yes After opening fixtures
Fix- fix 3 mm shell	32.82 Mpa	76.66Mpa	45.8 Mpa	No/ No neither during welding nor after opening fixtures

5-CONCLUSIONS

This work clearly shows that the proposed 3D analysis welding can predict not only the time but also the shape of buckling during welding. Also, one is able to see the behavior of the shell after buckling. In addition, the effect of external constraint and thickness on the buckling behavior due to welding are also studied. The global buckling was not seen in the fixed-fixed case before opening the fixtures but more local buckling occurred and finally, the shell buckled. The increase of thickness can eliminate both local and global bucklings.

REFERENCES

Argyris J H, Szimmat J, and William K J, 1982, "Computational aspects of welding stress analysis", Comput. Methods Appl. Mech. Engrg.,33, pp. 635-666.

Brown S B, Kim K H, and Anand L., 1989, "An Internal variable constitutive model for hot working of metals", International Journal of Plasticity,5, pp. 95-130

Hong J K, Tsai C L, and Dong P., 1998, "Assessment of numerical procedure for residual stress analysis in multi-pass welds", Welding Journal, pp. 372s-382s.

Masubuchi K. ,1980, "Analysis of welded structures", Pergamon Press, Oxford.

Murakawa H., Ueda Y. and Zhong X. M.,1995, "Buckling behavior of plates under idealized inherent strain", Transactions of JWRI, 24(2), pp. 87-91.

Michaleris P. and Debiccari A, 1997, "Prediction of welding distortion", Welding Journal, 76(4), pp. 172-180.

Michaleris P. and Debiccari A, 1996, "A predictive technique for buckling analysis of thin section panels due to welding", Journal of Ship Production, 12(4), pp. 269-275.

Michaleris P., Deo M.V. and Sun J., 2003, "Prediction of buckling distortion of welded structures", Science and Technology of Welding & Joining, 8(1), pp. 55-61.

Oddy A.S., Goldak J.A. and McDill J.M.J, 1990, "Numerical analysis of transformation plasticity in 3D finite element analysis of welds", European Journal of Mechanics,A/Solids,9(3), pp. 253-263.

Pattee F.M, 1975, "Buckling distortion of thin aluminium plates during welding", Thesis, Master of Science, Massachusetts Institute of Technology.

Ronda J, and Oliver GJ, 1998, "Comparison of applicability of various thermo-viscoplastic constitutive models in modeling of welding", Comput. Methods Appl. Mech. Engrg., 153, pp. 195-221.

Sarkani Sh, Tritchkov V, and Michaelov G., 2000, "An efficient approach for computing residual stresses in welded joints". Finite Elements in Analysis and Design, 35, pp. 247-268.

Tsai C.L., Park S.C. and Cheng W.T., 1999, "Welding distortion of a thin-plate panel structure", A.W.S., Welding Journal, Research Supplement, 78, pp. 156s-165s.

Watt D.F., Coon L., Bibby M. and Henwood C,1988."An algorithm for modeling microstructural development in weld heat affected zones (part a) reaction kinetics", Acta metal., 36(11),pp.3029-3035.